

A Monomeric Nickel–Dioxygen Adduct Derived from a Nickel(I) Complex and O<sub>2</sub>Koyu Fujita,<sup>†</sup> Ralph Schenker,<sup>‡</sup> Weiwei Gu,<sup>§</sup> Thomas C. Brunold,<sup>‡</sup> Stephen P. Cramer,<sup>§</sup> and Charles G. Riordan<sup>\*†</sup>*Department of Chemistry and Biochemistry, University of Delaware, Newark, Delaware 19716, Department of Chemistry, University of Wisconsin—Madison, Madison, Wisconsin 53706, and Department of Applied Science, University of California—Davis, Davis, California 95616*

Received January 30, 2004

The nickel(I) complex [PhTt<sup>Ad</sup>]Ni(CO) (PhTt<sup>Ad</sup>, phenyltris((1-adamantylthio)methyl)borate) reacts with O<sub>2</sub> generating a 1:1 species identified as a side-on dioxygen adduct based on its spectroscopic properties as supported by DFT computational results and by its reactivity. The Ni EXAFS data are fit to a S<sub>3</sub>O<sub>2</sub> coordination environment with short Ni–O distances, 1.85 Å. The brown complex displays a rhombic EPR signal with *g* values of 2.24, 2.19, 2.01. DFT and INDO/S-CI computations replicate the EXAFS and EPR features and suggest that **2** is a side-on [NiO<sub>2</sub>]<sup>+</sup> complex with geometric and electronic properties that are best rationalized in terms of a highly covalent Ni(II)–superoxo description. [PhTt<sup>Ad</sup>]-Ni(O<sub>2</sub>) oxidizes PPh<sub>3</sub> to OPPh<sub>3</sub>, NO to NO<sub>3</sub><sup>−</sup>, and [PhTt<sup>Bu</sup>]Ni(CO) to the nonsymmetric [PhTt<sup>Ad</sup>]Ni(μ-O)<sub>2</sub>Ni[PhTt<sup>Bu</sup>] dimer.

Nickel–dioxygen intermediates have been invoked in a number of stoichiometric and catalytic reactions. For example, nickel(II) azamacrocycles activate O<sub>2</sub> yielding products resulting from aromatic<sup>1</sup> and aliphatic<sup>2</sup> (ligand-based) C–H activation. Burrows has deployed related complexes as oxidative probes of the structure of proteins and DNA, albeit with more reactive oxidants, i.e., H<sub>2</sub>O<sub>2</sub> and KHSO<sub>5</sub>.<sup>3</sup> While metal-bound reduced dioxygen species have been suggested as the active reagents for these transformations, thorough characterization of the corresponding intermediates is generally lacking.<sup>4</sup> Recently, we reported that the Ni(I)

complex [PhTt<sup>Bu</sup>]Ni(CO) forms the purple dimer [(PhTt<sup>Bu</sup>)-Ni]<sub>2</sub>(μ-O)<sub>2</sub>, upon low-temperature exposure to O<sub>2</sub>.<sup>5,6</sup> Analogous bis-μ-oxo Ni<sub>2</sub>O<sub>2</sub> cores are accessible from Ni(II) precursors using H<sub>2</sub>O<sub>2</sub> as the oxidant.<sup>7</sup> To explore the mechanism by which the bis-μ-oxo dimer is generated from O<sub>2</sub> and to prepare intermediates that are more reactive toward exogenous substrates, we sought to redesign the [PhTt<sup>Bu</sup>] ligand so as to access a Ni(I) complex that would sterically preclude bis-μ-oxo dimer formation.<sup>8</sup> Herein, we report on the successful pursuit of this strategy which led to the discovery of a side-on dioxygen complex of nickel, shown to be an intermediate to bis-μ-oxo dimer formation.

Exposure of toluene or THF solutions of [PhTt<sup>Ad</sup>]Ni(CO), **1**,<sup>8</sup> to dioxygen produced a thermally sensitive, brown intermediate [PhTt<sup>Ad</sup>]Ni(O<sub>2</sub>), **2**, that formed with *k*<sub>obs</sub> = 8.4(6) × 10<sup>−3</sup> s<sup>−1</sup> (toluene, −70 °C), Scheme 1. The composition of **2** was deduced by its unique spectroscopic features<sup>9</sup> and supported by its reactivity. The optical spectrum of **2** in THF exhibits bands at λ<sub>max</sub> (ε [M<sup>−1</sup> cm<sup>−1</sup>]) 310 (5900), 386 (2900), 450 (2500), and 845 (350) nm. In the UV region the spectrum is strikingly similar to those of Co<sup>10</sup> and Cu<sup>11,12</sup> side-on dioxygen complexes. In contrast, [(PhTt<sup>Bu</sup>)Ni]<sub>2</sub>(μ-O)<sub>2</sub> dis-

\* Author to whom correspondence should be addressed. E-mail: riordan@udel.edu.

<sup>†</sup> University of Delaware.

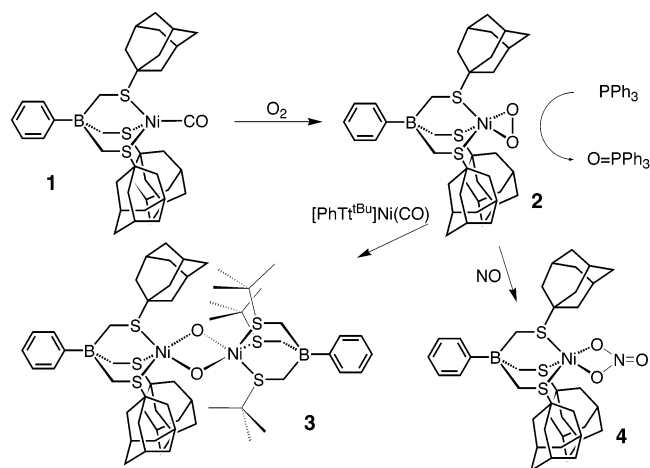
<sup>‡</sup> University of Wisconsin—Madison.

<sup>§</sup> University of California—Davis.

- (1) (a) Kimura, E.; Sakonaka, A.; Machida, R. *J. Am. Chem. Soc.* **1982**, *104*, 4255–4257. (b) Kimura, E.; Machida, R. *J. Chem. Soc., Chem. Commun.* **1984**, 499–500. (c) Kushi, Y.; Machida, R.; Kimura, E. *J. Chem. Soc., Chem. Commun.* **1985**, 216–218.
- (2) (a) Chen, D.; Martell, A. E. *J. Am. Chem. Soc.* **1990**, *112*, 9411–9412. (b) Cheng, C.-C.; Gulia, J.; Rokita, S. E.; Burrows, C. J. *J. Mol. Catal. A.* **1996**, *113*, 379–391. Berkessel, A.; Bats, J. W.; Schwarz, C. *Angew. Chem., Int. Ed. Engl.* **1990**, *29*, 106–108.
- (3) (a) Muller, J. G.; Hickerson, R. P.; Perez, R. J.; Burrows, C. J. *J. Am. Chem. Soc.* **1997**, *119*, 1501–1506. (b) Burrows, C. J.; Perez, R. J.; Muller, J. G.; Rokita, S. E. *Pure Appl. Chem.* **1998**, *70*, 275–278.

- (4) A noteworthy exception is the side-on Ni(II)–peroxo complex, (RNC)<sub>2</sub>Ni(O<sub>2</sub>), accessed via the Ni(0)/Ni(II) couple: Otsuka, S.; Nakamura, A.; Tatsuno, Y. *J. Am. Chem. Soc.* **1969**, *91*, 6994–6999.
- (5) [PhTt<sup>Bu</sup>], phenyltris(*tert*-butylthio)methylborate. Mandimutsira, B. S.; Yamarik, J. L.; Brunold, T. C.; Gu, W.; Cramer, S. P.; Riordan, C. G. *J. Am. Chem. Soc.* **2001**, *123*, 9194–9195.
- (6) Schenker, R.; Mandimutsira, B. S.; Riordan, C. G.; Brunold, T. C. *J. Am. Chem. Soc.* **2002**, *124*, 13842–13855.
- (7) (a) Hikichi, S.; Yoshizawa, M.; Sasakura, Y.; Akita, M.; Moro-oka, Y. *J. Am. Chem. Soc.* **1998**, *120*, 10567–10568. (b) Itoh, S.; Bandoh, H.; Nagatomo, S.; Kitagawa, T.; Fukuzumi, S. *J. Am. Chem. Soc.* **1999**, *121*, 8945–8946. (c) Shiren, K.; Ogo, S.; Fujinami, S.; Hayashi, H.; Suzuki, M.; Uehara, A.; Watanabe, Y.; Moro-oka, Y. *J. Am. Chem. Soc.* **2000**, *122*, 254–262. (d) Hikichi, S.; Yoshizawa, M.; Sasakura, Y.; Komatsuzaki, H.; Moro-oka, Y.; Akita, M. *Chem. Eur. J.* **2001**, *7*, 5011–5028. (e) Itoh, S.; Bandoh, H.; Nakagawa, M.; Nagatomo, S.; Kitagawa, T.; Karlin, K. D.; Fukuzumi, S. *J. Am. Chem. Soc.* **2001**, *123*, 11168–11178.
- (8) [PhTt<sup>Ad</sup>], phenyltris((1-Adamantylthio)methyl)borate. Fujita, K.; Rheingold, A. L.; Riordan, C. G. *J. Chem. Soc., Dalton Trans.* **2003**, 2004–2008.
- (9) See Supporting Information for full spectroscopic and computational details.

Scheme 1



plays intense features at 410 nm ( $\epsilon = 6000 \text{ M}^{-1} \text{ cm}^{-1}$  per Ni) and 565 nm (8000), the latter ascribed to a O $\rightarrow$ Ni charge transfer (CT) transition.<sup>6</sup> The electrospray ionization mass spectrum of **2** reveals a positive ion cluster at  $m/z$  of 705. The isotope distribution pattern agrees with that calculated for a species of empirical formula  $[\text{PhTt}^{\text{Ad}}\text{Ni}(\text{O})]^+$ . Furthermore, the signal shifts to higher mass by two units for samples of **2** derived from <sup>18</sup>O<sub>2</sub>. The isotope-sensitive ion signals confirm that oxygen is a constituent of the complex, although there is no indication of the parent ion in the mass spectrum.

**2** displays paramagnetically shifted <sup>1</sup>H NMR spectral resonances and an  $S = 1/2$  EPR spectrum at 4.2 K.<sup>9</sup> The rhombic signal with  $g$  values of 2.24, 2.19, and 2.01 supports the monomeric formulation and is indicative of a ( $d_{z^2}$ )<sup>1</sup> electron configuration typically observed for Ni(III) species.<sup>13</sup> The Ni coordination sphere has been characterized by Ni K edge X-ray absorption spectroscopy (XAS). A preedge 1s  $\rightarrow$  3d transition occurs at 8331.4 eV, a value 1 eV greater than that for the Ni(I) precursor, **1**, but 1 eV lower than observed in the Ni(III)<sub>2</sub> dimer,  $[(\text{PhTt}^{\text{tBu}}\text{Ni}]_2(\mu\text{-O})_2$ , thus suggesting a Ni(II) oxidation state.<sup>5</sup> The Ni EXAFS data corroborate the monomeric nature of **2**, Figure 1. Specifically, there is no indication of a short M—M vector as observed for  $[(\text{PhTt}^{\text{tBu}}\text{Ni}]_2(\mu\text{-O})_2$  and deemed diagnostic of bis- $\mu$ -oxo rhombs.<sup>14</sup> The Ni ligation consists of three sulfur atoms at Ni—S<sub>av</sub>, 2.26 Å, and two oxygen atoms at Ni—O<sub>av</sub>, 1.85 Å. The latter value is in the range found by X-ray diffraction for M—O distances in side-on O<sub>2</sub> complexes.<sup>10,12,15</sup> Although the accuracy of coordination number assignment by EXAFS

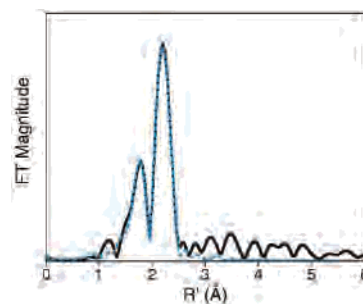


**Figure 1.** Fourier transform of EXAFS data (solid black line) and simulation (dashed blue line) for **2** ( $k$ , 2–16.5 Å<sup>-1</sup>). Simulation: 3 S at 2.26 Å ( $\sigma^2$ , 0.03) and 2 O at 1.85 Å (0.03).

is limited, the data are fit much better assuming two O ligands rather than one, consistent with a side-on coordination of the dioxygen ligand. Side-on vs end-on O<sub>2</sub> coordination could in principle be distinguished spectroscopically via vibrational analysis of the <sup>16</sup>O/<sup>18</sup>O isotopomer.<sup>10,11,16</sup> However, resonance Raman spectroscopic experiments on **2** have failed to identify oxygen-isotope sensitive bands, presumably due to the low intensity of the optical features associated with the  $[\text{NiO}_2]^+$  unit.

To further corroborate the structural assignment of **2**, a computational analysis of hypothetical side-on and end-on O<sub>2</sub> complexes (possessing a suitably truncated derivative of the PhTt<sup>Ad</sup> ligand)<sup>9</sup> was undertaken. The two models were energy minimized by DFT using the B3LYP hybrid functional,<sup>17</sup> and for the optimized structures the  $g$  values were obtained from semiempirical INDO/S-CI computations as implemented in ORCA.<sup>9,18</sup> These calculations yielded principal  $g$  values of 2.29, 2.22, and 2.09 for the side-on O<sub>2</sub> complex and 2.44, 2.33, and 2.21 for the end-on complex. While the former values are consistent with the EPR data, the latter are considerably too high, arguing against the presence of an end-on bound O<sub>2</sub> moiety in **2**. In further support of a side-on O<sub>2</sub> description of **2**, calculated <sup>17</sup>O hyperfine coupling constants for this model indicate very little unpaired spin density on the O<sub>2</sub> ligand, which concurs nicely with the observation that the EPR spectrum of **2** prepared with <sup>17</sup>O<sub>2</sub> shows no resolvable coupling.<sup>9</sup> The side-on structure is square pyramidal, high-spin Ni(II) with two sulfurs and two oxygens in the basal plane and the remaining sulfur in the apical position (Figure 2a, left). The calculated average Ni—S and Ni—O bond distances of 2.33 and 1.87 Å, respectively, are in good agreement with those determined by EXAFS spectroscopy, while the computed O—O bond length of 1.38 Å appears characteristic of a peroxo spe-

(10) Egan, J. W., Jr.; Haggerty, B. S.; Rheingold, A. L.; Sendlinger, S. C.; Theopold, K. H. *J. Am. Chem. Soc.* **1990**, *112*, 2445–2446.  
 (11) Fujisawa, K.; Tanaka, M.; Moro-oka, Y.; Kitajima, N. *J. Am. Chem. Soc.* **1994**, *116*, 12079–12080.  
 (12) Spencer, D. J. E.; Aboelella, N. W.; Reynolds, A. M.; Holland, P. L.; Tolman, W. B. *J. Am. Chem. Soc.* **2002**, *124*, 2108–2109.  
 (13) Spectral characteristics of  $[\text{PhTt}^{\text{tBu}}\text{Ni}(\text{O}_2)]$ : UV-vis (toluene) 310 nm, 390 nm, 450 nm; EPR (toluene, 20 K)  $g$  values 2.24, 2.20, 2.02.  
 (14) Que, L.; Tolman, W. B. *Angew. Chem., Int. Ed.* **2002**, *41*, 1114–1137.  
 (15) (a) Kitajima, N.; Komatsuzaki, H.; Hikichi, S.; Osawa, M.; Moro-oka, Y. *J. Am. Chem. Soc.* **1994**, *116*, 11596–11597. (b) Cramer, C. J.; Tolman, W. B.; Theopold, K. H.; Rheingold, A. L. *Proc. Natl. Acad. Sci. U.S.A.* **2003**, *100*, 3635–3640.

(16) (a) Kurtz, D. M.; Shriver, D. F.; Klotz, I. M. *J. Am. Chem. Soc.* **1976**, *98*, 5033–5035. (b) Pate, J. E.; Cruse, R. W.; Karlin, K. D.; Solomon, E. I. *J. Am. Chem. Soc.* **1987**, *109*, 2624–2630. (c) Chaudhuri, P.; Hess, M.; Weyhermüller, T.; Wieghardt, K. *Angew. Chem., Int. Ed.* **1999**, *38*, 1095–1098.  
 (17) The minimized energy for the side-on complex is 10.0 kcal/mol lower than that for the end-on complex.  
 (18) Neese, F.; Max Planck Institute for Radiation Chemistry, Mülheim/Ruhr, Germany; neese@mpi-muelheim.mpg.de. For information regarding the accuracy of  $g$  values computed by the INDO/S-CI method, see: (a) Neese, F. *Curr. Opin. Chem. Biol.* **2003**, *7*, 125–135. (b) Neese, F.; Solomon, E. I. *Inorg. Chem.* **1998**, *37*, 6568–6582. (c) Neese, F.; Zaleski, J. M.; Loeb-Zaleski, K. E.; Solomon, E. I. *J. Am. Chem. Soc.* **2000**, *122*, 11703–11724.

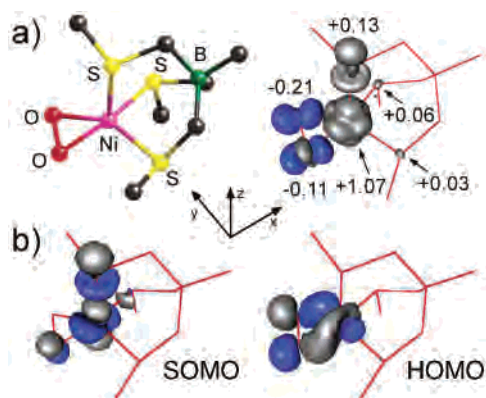


**Figure 2.** (a) Geometric structure (left) and total unpaired spin density distribution (right). Unpaired spin densities on individual atoms are indicated. The coordinate system is defined by the  $g$  matrix orientation as obtained from INDO/S-CI computations. (b) Key natural orbitals of **2** as obtained from spin-unrestricted DFT computations.

cies.<sup>19,20</sup> However, as DFT computations on peroxo species typically yield O–O bond lengths greater than 1.4 Å,<sup>15b</sup> this result actually agrees well with the XAS data, also indicating that **2** possesses substantial Ni(II)–superoxo character. Nonetheless, the DFT-computed total unpaired spin density for **2** is predominantly located on the Ni center (Figure 2a, right). These findings suggest an electronic structure in which the unpaired electron in the Ni  $d_{x^2-y^2}$  orbital and the  $O_2^-$  radical are strongly antiferromagnetically coupled, consistent with the fact that the HOMO (Figure 2b) possesses nearly identical contributions from the Ni  $d_{x^2-y^2}$  and the in-plane  $O_2^- \pi^*$  orbitals. The remaining single unpaired electron resides primarily in the Ni  $d_z^2$  orbital (SOMO, Figure 2b), which explains the general features of the EPR spectrum and the lack of sizable hyperfine broadening in samples of **2** prepared with  $^{17}O_2$ . A similar model has been invoked to explain the EPR properties of {FeNO}<sup>7</sup> systems, for which detailed studies by Solomon and co-workers revealed that the observed  $S = 3/2$  ground state arises from strong antiferromagnetic coupling between the Fe(III) center ( $S = 5/2$ ) and  $NO^-$  ( $S = 1$ ).<sup>21</sup> Together, the spectroscopic and computational results suggest that **2** is a side-on  $[NiO_2]^+$  complex with geometric and electronic properties that are consistent with a formal Ni(II)–superoxo description.<sup>19,20</sup>

(19) Gubelmann, M. H.; Williams, A. F. *Struct. Bonding (Berlin)* **1983**, 55, 1.

(20) Alternatively, the computed O–O distance of 1.29 Å for the end-on model of **2** indicates that this isomer has predominantly Ni(II)–superoxo character, consistent with the DFT calculated spin densities for that model (Table 3S).

(21) Zhang, Y.; Pavlosky, M. A.; Brown, C. A.; Westre, T. E.; Hedman, B.; Hodgson, K. O.; Solomon, E. I. *J. Am. Chem. Soc.* **1992**, 114, 9189–9191. Brown, C. A.; Pavlosky, M. A.; Westre, T. E.; Zhang, Y.; Hedman, B.; Hodgson, K. O.; Solomon, E. I. *J. Am. Chem. Soc.* **1995**, 117, 715–732.

Preliminary exploration indicates the reactivity of **2** to be rich, Scheme 1. Unlike  $[(PhTt^{tBu})Ni]_2(\mu-O)_2$ , **2** transfers an equivalent of oxygen to  $PPh_3$ , generating  $OPPh_3$  quantitatively;  $^{18}O$  labeling confirms  $O_2$  as the source. The electrophilic character of **2** is reminiscent of reactivity observed for a Ni(II)–peroxo adduct.<sup>22</sup> **2** oxidizes nitric oxide to nitrate forming  $[PhTt^{Ad}]Ni(NO_3)$  (the nitrite complex,  $[PhTt^{Ad}]Ni(NO_2)$  is a minor (15%) product;  $^1H$  NMR spectral quantitation and comparison with authentic samples). More interestingly, **2** reacts with the smaller Ni(I) precursor,  $[PhTt^{tBu}]Ni(CO)$ , forming the corresponding purple bis- $\mu$ -oxo dimer, **3** (85% yield), with different borato ligands on each Ni.<sup>23</sup> Also, oxygenation of  $[PhTt^{tBu}]Ni(CO)$  proceeds initially to an intermediate with optical and EPR spectral parameters similar those observed for **2**.<sup>13</sup> The short-lived  $[PhTt^{tBu}]Ni(O_2)$  decays, yielding  $[(PhTt^{tBu})Ni]_2(\mu-O)_2$ . These observations indicate that **2** and the related side-on  $O_2$  complex,  $[PhTt^{tBu}]Ni(O_2)$ , are bona fide intermediates in bis- $\mu$ -oxo Ni(III)<sub>2</sub> dimer formation.

In summary, spectroscopic analysis of the thermally sensitive brown intermediate, **2**, produced from dioxygen supports the structural assignment of a side-on dioxygen adduct best described as a Ni(II)–superoxo complex in which the superoxide radical is antiferromagnetically coupled to the high-spin Ni(II) center to yield an  $S = 1/2$  EPR spectrum characteristic of a  $d_z^2$  ground state electronic configuration. Electronic structure calculations provide strong support for the side-on coordination mode as the calculated EPR  $g$  values and metric parameters agree well with those determined experimentally.<sup>9</sup> The reactivity of **2** points to an  $O_2$  adduct that is competent to transfer  $O_2$  to NO and an O atom to  $PPh_3$ . **2** is an intermediate in bis- $\mu$ -oxo Ni(III)<sub>2</sub> dimer generation provided the sulfur substituents of its Ni(I) reaction partner are sufficiently small so as to allow for close approach of two metals.

**Acknowledgment.** We thank the National Science Foundation (C.G.R.), the University of Wisconsin and the Sloan Research Foundation (T.C.B.), and the Swiss National Science Foundation (R.S.) for financial support and Dr. Frank Neese (MPI Mülheim), Profs. Brian Hoffman (Northwestern), and Ed Solomon (Stanford) for useful discussions.

**Supporting Information Available:** Synthetic procedures along with computational and characterization data (PDF). This material is available free of charge via the Internet at <http://pubs.acs.org>.

IC049876N

(22) Otsuka, S.; Nakamura, A.; Tatsuno, Y.; Miki, M. *J. Am. Chem. Soc.* **1972**, 94, 3761–3767.

(23) A similar strategy yielded the  $LCu(\mu-O)_2CuL'$  complexes: Aboeella, N. W.; Lewis, E. A.; Reynolds, A. M.; Brennessel, W. W.; Cramer, C. J.; Tolman, W. B. *J. Am. Chem. Soc.* **2002**, 124, 10660–10661.